A HYBRID QUANTUM-CLASSICAL CNN ARCHITECTURE FOR SEMANTIC SEGMENTATION OF RADAR SOUNDER DATA

Raktim Ghosh^{1,2}, Amer Delilbasic^{3,4,5}, Gabriele Cavallaro^{3,4}, Francesca Bovolo²

University of Trento, Italy, and ² Fondazione Bruno Kessler, Trento, Italy
 Jülich Supercomputing Centre, Forschungszentrum Jülich, Germany
 School of Engineering and Natural Sciences, University of Iceland, Iceland
 Φ-lab, ESRIN, European Space Agency, Italy

ABSTRACT

The article presents for the first time a hybrid quantum-classical architecture in the context of subsurface target detection in the radar sounder signal. We enhance the classical convolutional neural network (CNN) based architecture by integrating a quantum layer in the latent space. We investigate two quantum circuits with the classical neural networks by exploiting fundamental properties of quantum mechanics such as entanglement and superposition. The proposed hybrid architecture is used for the downstream task of patch-wise semantic segmentation of radar sounder subsurface images. Experimental results on the MCoRDS and MCoRDS3 datasets demonstrated the capability of the hybrid quantum-classical approach for radar sounder information extraction.

Index Terms— radar sounder, quantum computing, quantum machine learning, subsurface sensing, segmentation

1. INTRODUCTION

Radar Sounders are nadir-looking instruments equipped with active sensing capabilities that transmit linearly modulated EM pulses and receive the backscattered echoes from subsurface targets depending on the geophysical properties such as dielectric discontinuities, target geometry, etc. The operating range of these sensors varies from High Frequency (HF) to Very High Frequency (VHF) bands [1]. The backscattered returns are coherently summed, Synthetic Aperture Radar (SAR) focused, and post-processed by clutter reduction, platforms instability correction, etc., to generate radargrams (see Figure 1). The radargrams can be exploited for miscellaneous subsurface investigations, subsurface target detection, segmentation, estimation of geophysical properties, etc. Research activities have been carried out on classical machine learning for radargrams information extraction by Convolutional Neural Network (CNN) or Transformer-based methods. These

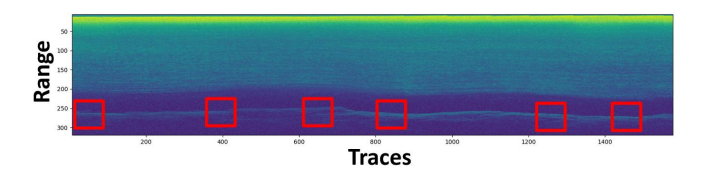


Fig. 1. A Sample MCoRDS Radargram. Red blocks are the patches extracted for training and testing the HQC architecture. approaches include both supervised [2] and unsupervised [3] segmentation techniques and showed good performance. Over the last few years, Quantum Machine Learning (QML) has emerged as an interdisciplinary field with a view to improving the computational tasks of classical machine learning models by leveraging quantum algorithms to incorporate in Quantum Computers [4]. However, no work has been carried out so far in the context of QML architectures for characterizing radargrams.

In the last few years, a substantial amount of research activities have been carried out in the development of different types of Quantum Computers [4]. Quantum Computers incorporate the principle of quantum mechanics to perform computations using qubits. After the quantum measurement, the superposition state of a qubit is either collapsed to the basis states $|0\rangle$ or $|1\rangle$, according to the corresponding probabilities. For every n qubits, we can represent 2^n possible states, thereby demonstrating the exponential improvement in respect of the classical bits. By utilizing principles of QC, quantum algorithms are developed to address miscellaneous computational problems ranging from search and optimizations, quantum simulations, quantum cryptography, etc [4]. In remote sensing image classification, [5] incorporated Quantum SVM based on quantum annealing and [6] developed gate-based QC with Hybrid Quantum-Classical (HQC) architecture. Recently, [7] developed a HQC architecture by utilizing the quantum circuits as feature extractors for multi-spectral Sentinel-2 images and classical architecture for final predictions. However, there is no attempt to use quantum related concepts in processing radar sounder.

This study aims to explore the potential of QC in the

This work was supported by the Italian Space Agency through the "Missione JUICE - Attività dei team scientifici dei Payload per Lancio, commissioning, operazioni e analisi dati" Agenzia Spaziale Italian-Istituto Nazionale di Astrofisica (ASI-INAF), under Contract 2023-6-HH.0.

context of radar sounder image segmentation. We develop a HQC architecture by extending the hybrid framework of [6] for the task of patch-wise semantic segmentation. We utilize the Quantum Circuit in the latent space of a UNET-like architecture for transferring discriminative contexts between the encoder and decoder. Experimental results demonstrated the potential of Quantum Circuits to establish a contextually rich information processing system in the latent space of HQC architecture. However, the similar contextual richness was not observed while replacing the Quantum Circuits with the classical fully connected (FC) layers during training. Therefore, Quantum Circuits turned out to be a stable bottleneck connector as opposed to the FC layers for the similar architectural settings.

2. PROPOSED METHODOLOGY

The overall goal of the proposed HQC architecture is to classify each pixel in the radargram patches into distinct classes.

Figure 3 shows the HQC architecture for the semantic segmentation of the radar sounder data. At first, the successive convolutional layers are used to encode the information to a higher dimensional discriminative embedding space. The intermediate feature tensors are flattened to a specified dimension, and the FC layers are introduced to reduce the dimensionality of the feature tensors to the number of parameters in the quantum circuits. The classical information at the last bottleneck layer in the Encoder is injected into the parameterized quantum circuits. After the measurement is performed on the *qubits*, the corresponding probability amplitudes are utilized as an input to the Decoder. The Decoder upsamples the input spatial dimension for the final patch-wise predictions.

2.1. HQC Encoder

The Encoder performs convolution operations with window size of $w \times w$, and max-pooling operations reduce the spatial dimension of the input tensor from $[H \times W]$ to $[\frac{H}{2^3} \times \frac{W}{2^3}]$ using the sequence as $[\frac{H}{2^j} \times \frac{W}{2^j}]$, where $j \in \{1, 2, ..., \lambda\}$. The CNN embeds high dimensional local spatial contexts on feature tensors. The dimensionality of tensors extracted from CNN is reduced to the number of parameters expected in the quantum layers in the bottleneck. Let us denote a feature tensor (derived from a training sample through CNN embedding, upper branch in Fig. 3) as $\theta = \{\theta_0, \theta_1, ..., \theta_K\}$ where K is the number of parameters in the quantum circuit.

2.2. HQC Bottleneck Quantum Layer

 $\{\theta_0, \theta_1, ..., \theta_K\}$ is injected into the quantum circuit (QC in Fig. 3) made of rotation gates to estimate probability amplitudes with respect to the basis states of a 4-qubit system bottleneck quantum layer for the proposed HQC architecture. To simplify the explanation for the quantum circuits, we elucidate on 2-qubit quantum system.

A. Two-Qubit Quantum System

Let us consider a 2-qubit system with the respective state space $|\psi_0\rangle = \alpha_0 |0\rangle + \beta_0 |1\rangle$ and $|\psi_1\rangle = \alpha_1 |0\rangle + \beta_1 |1\rangle$ with $|\alpha_0|^2 + |\beta_0|^2 = 1$ and $|\alpha_1|^2 + |\beta_1|^2 = 1$ with α_0 , α_1 and β_0 , β_1 representing the probability of measuring corresponding states $|0\rangle$ and $|1\rangle$, respectively. The joint evolution of the 2-qubit system with states $|\psi_0\rangle$ and $|\psi_1\rangle$ can be denoted as $|\psi_0\rangle \otimes |\psi_1\rangle$ (or $|\psi_0\psi_1\rangle$). The composite representation of the states $|\psi_0\rangle$ and $|\psi_1\rangle$, is:

$$|\psi_0\rangle \otimes |\psi_1\rangle = \alpha_0\alpha_1 |00\rangle + \alpha_0\beta_1 |01\rangle + \beta_0\alpha_1 |10\rangle + \beta_0\beta_1 |11\rangle$$
(1)

where $\alpha_i, \beta_j \in \mathbb{C}$, and $\alpha_0\alpha_1 + \alpha_0\beta_1 + \beta_0\alpha_1 + \beta_0\beta_1 = 1$. Let us consider a state in which $|\psi\rangle = \frac{1}{\sqrt{2}}|00\rangle + \frac{1}{\sqrt{2}}|11\rangle$. To factorize states of two qubits, probabilities in Eq. 1 has to be as $\alpha_0\alpha_1 = \frac{1}{\sqrt{2}}, \alpha_0\beta_1 = 0, \beta_0\alpha_1 = 0, \beta_0\beta_1 = \frac{1}{\sqrt{2}}$, which is contradictory in terms of feasible solutions. Therefore, $|\psi\rangle$ cannot be factorized into the product states of two qubits. This phenomenon is known as Entanglement. The state $|\psi\rangle$ is also known as Bell state $|\psi\rangle_{Bell}$:

$$|\psi\rangle_{Bell} = \frac{1}{\sqrt{2}}|00\rangle + \frac{1}{\sqrt{2}}|11\rangle \tag{2}$$

If the measurement on the first qubit collapses to state $|0\rangle$ with a probability of 0.5, the entangled state will collapse to $|00\rangle$. The state of the second qubit will be automatically $|0\rangle$. If two qubits are separated after Entanglement, the results hold true for even a theoretically infinite separation of two qubits, thus violating the classical locality principles. Also, several experiments on measuring the properties of the entangled particles separated at a distance, violated the Bell's inequality. The reader is referred to [8] for further details on the mathematical treatment.

B. Quantum Gates

The language of Quantum Computation can be described through the changes occurring over the quantum states. Analogous to the classical computer with logic gates, a quantum computer is built with Quantum Gates to carry out quantum information processes by manipulating these gates. Quantum gates perform unitary operations with $U^{\dagger}U = UU^{\dagger} = I$, where \dagger is the conjugate transpose operator on the unitary matrix U.

The *Hadamard Gate* is described by the following equation.

$$H = \frac{1}{\sqrt{2}} \begin{pmatrix} 1 & 1\\ 1 & -1 \end{pmatrix} \tag{3}$$

If we consider a qubit with state $|0\rangle$, the Hadamard Gate will return the superposition of two states

$$H|0\rangle = \frac{1}{\sqrt{2}} \begin{pmatrix} 1 & 1\\ 1 & -1 \end{pmatrix} \begin{pmatrix} 1\\ 0 \end{pmatrix} = \frac{1}{\sqrt{2}} \begin{pmatrix} 1\\ 1 \end{pmatrix} = \frac{1}{\sqrt{2}} \begin{pmatrix} 1\\ 0 \end{pmatrix} + \frac{1}{\sqrt{2}} \begin{pmatrix} 0\\ 1 \end{pmatrix}$$
 (4)

The Hadamard Gates are also attributed as "square-root of NOT" gate as it turns a state $|0\rangle$ into $(|0\rangle + |1\rangle)/\sqrt{2}$.

The *Rotation Gates* (denoted as $R_x(\theta)$, $R_y(\theta)$, $R_z(\theta)$) are single qubit gates described by the rotation operations on the Bloch sphere with the rotation along the x, y, and z axis with the angle θ . In particular, the Gate $R_y(\theta)$ is described in the following form:

$$R_{y}(\theta) = \begin{pmatrix} \cos(\frac{\theta}{2}) & -\sin(\frac{\theta}{2}) \\ \sin(\frac{\theta}{2}) & \cos(\frac{\theta}{2}) \end{pmatrix}$$
 (5)

The *Controlled-NOT* Gate transforms the composite state $\alpha_0\alpha_1|00\rangle + \alpha_0\beta_1|01\rangle + \beta_0\alpha_1|10\rangle + \beta_0\beta_1|11\rangle$ (2) into $\alpha_0\alpha_1|00\rangle + \alpha_0\beta_1|01\rangle + \beta_0\alpha_1|11\rangle + \beta_0\beta_1|10\rangle$. CNOT gates are utilized to create entangled or disentangled states.

$$U = \begin{pmatrix} 1 & 0 & 0 & 0 \\ 0 & 1 & 0 & 0 \\ 0 & 0 & 0 & 1 \\ 0 & 0 & 1 & 0 \end{pmatrix} \tag{6}$$

By utilizing the Hadamard Gate and the CNOT gate, a *Bell state* can be created in the following way. At first the composite state with 2-qubit system $|0\rangle\otimes|0\rangle$ is prepared. If the Hadamard gate operates on the first qubit, the superposition of the state becomes $\frac{1}{\sqrt{2}}(|0\rangle+|1\rangle)$. Therefore, the composite state will be $\frac{1}{\sqrt{2}}(|00\rangle+|10\rangle)$. After the CNOT gate, the final state after the quantum circuit will be $\frac{1}{\sqrt{2}}(|00\rangle+|11\rangle)$, thereby creating an entangled state.

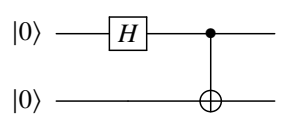


Fig. 2. A Quantum Circuit to create Bell State

B. Quantum Circuits

In this section, we elucidate the two standard quantum circuits from the IBM Qiskit framework which are utilized as HQC bottleneck quantum layer.

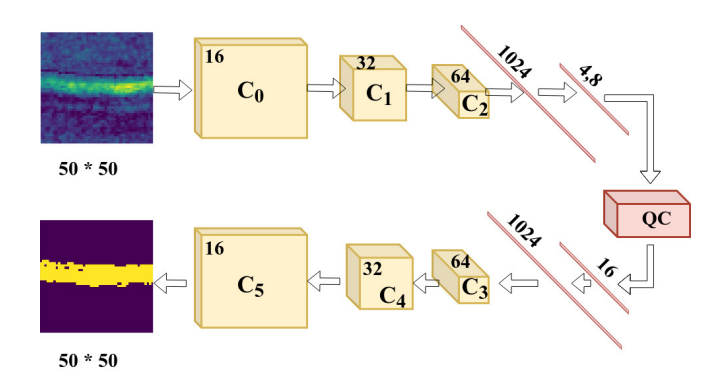


Fig. 3. Hybrid Quantum-Classical Neural Network.

1. Bellman Quantum Circuit

The first circuit is the Bellman Quantum Circuit as shown in Fig 4. Initially, the circuit prepares an entangled state by utilizing the Hadamard and CNOT gates. This phenomenon can be attributed to quantum correlations. After establishing the entanglement, the parameterized rotation gates are incorporated into the entangled state. All the qubits are rotated along the y-axis with parameters θ that correspond to the embeddings in output to the CNN bottleneck. The angular units in the rotation gates are parameterized by the classical information. After the rotated entangled states, the consecutive CNOT processes are mirrored with respect of the preceding CNOT operations while creating the entangled state. Overall, the classical information θ derived from the classical networks is transformed into the quantum feature space by utilizing the entanglement and superposition on the Bellman circuit. As the circuit creates an entangled state along with the rotation gates, this transformation seems to amplify the classical information into the quantum feature spaces more efficiently.

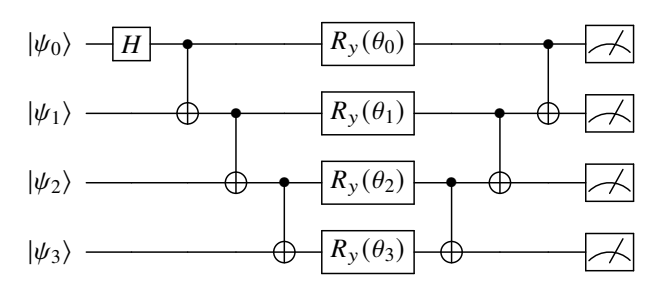


Fig. 4. Schematic Layout of the Bellman Quantum Circuit.

2. Real Amplitudes Circuit

The second circuit is the Real Amplitude circuits as shown in Fig 5. At first, all the qubits are passed through corresponding Hadamard Gates and then the rotation gates are incorporated in the joint state of the system with parameters θ . Hereafter, by utilizing the CNOT gates, the mutual entanglements are established between the *qubits*. After that, four rotation gates are incorporated with parameters θ_i . The advantages of the Real Amplitudes circuit seems to lie in encoding the classical information before and after the Entanglement of the Qubits.

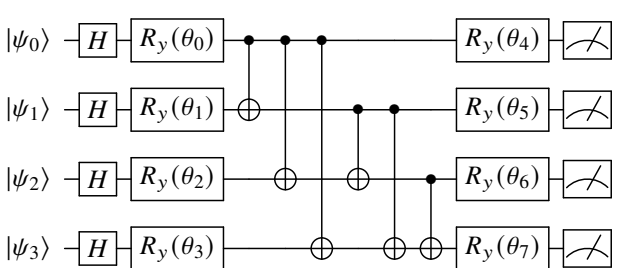


Fig. 5. Schematic Layout of the Real Amplitudes Circuit.

C. Quantum Embedding

We integrate a parameterized quantum circuit as a hidden layer of the HQC neural network. To embed the classical data for the parameterization on quantum circuits, a higher dimensional classical feature mapping is important to enhance the contextual richness w.r.t depth of the network. By utilizing the unitary operators over the quantum nodes, a quantum feature mapping is performed over the high dimensional classical encoding. To inject the classical information into the quantum circuit by utilizing the unitary operators, the classical information has to be passed through high dimensional discriminative feature embedding through miscellaneous layers of activation. Here, we utilize the successive CNN layers. After injecting the values $\{\theta_1, \theta_2, ..., \theta_K\}$ into the quantum circuits, the sequence of measured probability amplitudes for the 4 - qubit system can be denote as $\{p_1, p_2, ..., p_{2^4}\}$. This sequence is utilized in the decoder architecture for the final predictions (see Section 2.3). It is worth mentioning that we can utilize different quantum gates (such as rotation gates, Hadamard gates, etc.) to encode classical information.

2.3. HQC Decoder

The decoder takes probability amplitudes $\{p_1, p_2, ..., p_{2^4}\}$ as input which are fed into the FC layers by projecting the amplitudes to a higher dimensional feature space. The corresponding feature tensors are then reshaped for the successive convolution operations. By incorporating the successive Transpose Convolution operations, the spatial dimension [H, W] is recovered for predictions.

3. EXPERIMENTAL RESULTS

3.1. Dataset

We tested our HQC architecture on the MCoRDS and MCoRDS3 datasets hosted by the Centre of Remote Sensing of Ice Sheets (CReSIS) unit. The operating bandwidths of MCoRDS are 9.5 MHz and 30 MHz. The operating altitude of the aircraft was 7000 m. The campaign took place over several locations of Antarctica ranging from (-86°00′N to -15°67′E) to (-86°02′N to 29°45′E) on November 2010. A total trace of 400 line-km is covered along the azimuth direction with 27350 range lines for the MCoRDS dataset. In the case of the MCoRDS3 dataset, the operating bandwidth is 30 MHz, with the Aircraft altitude of about 500m. The total number of range lines for the MCoRDS3 dataset is 30009. The campaign for the MCoRDS3 dataset took place in inland Greenland in 2017.

3.2. Experimental Setup

The radargrams are labeled along the azimuth and range directions according to the different targets. We extracted the patches from the MCoRDS and MCoRDS3 datasets. The labelled targets are ice layers, bedrock, and noise across the range directions. Here we focus on distinguishing the noise and bedrock. We extracted patches from the radargram across

 Table 1. Accuracy Assessment

Algorithms	F1-Score	OA
HQC (Real Amplitudes Circuit)	0.8477	93.93
HQC (Bellman Circuit)	0.8248	93.13
Classical Architecture	0.7407	89.55

the width of the bedrock along with the noise. The spatial dimension of each training sample is $H \times W = 50 \times 50$. We utilize 800 samples for training and 254 samples for testing. We incorporate convolution operations (Kernel Size is $w \times w$ $= 3 \times 3$), along with the downsampling with max pooling followed by ReLU activation. λ is set to 3. The downsampling operation reduced the spatial dimension from 50×50 to 4×4 . After that, the convolution blocks are flattened with a spatial dimension of $4 \times 4 \times 64 = 1024$. The MLP was utilized to reduce the dimension from 1024 to 4 (for Bellman Circuit) and 8 (for Real Amplitudes Circuit), according to the number of parameters associated to quantum circuit. The Bellman and Real Amplitudes Quantum Circuits are considered hidden quantum layers. These 4 and 8 classical values derived from the last fully connected layer in the Encoder are injected into the parameterized rotation gates of the corresponding quantum circuits. The quantum circuits are 4 - qubits quantum systems. We incorporate IBM AerSimulator as a backend simulator on the Qiskit framework with 512 shots for estimating the probabilities corresponding to distinct basis vectors. We utilize the Pytorch and Qiskit framework to implement the HQC architecture. The training iterations are kept as 100 with the learning rate 1e - 5 while taking the batch size as 16. We utilize the F1-score and Overall Accuracy as evaluation metrics.

3.3. Segmentation Results

In this section, we report the quantitative (see Figure 6) and qualitative (see Table 1) assessment of the proposed HQC architecture by utilizing the Bellman circuit and Real Amplitude Circuits as a hidden quantum layer. A comparative analysis is performed with the classical counterpart of the HQC architecture. Notice that, for the classical counterpart, we discard the hidden quantum layer and integrate the Encoder and Decoder with the fully connected layers as a bottleneck in the latent space. Quantitatively, the proposed architecture with the Real Amplitude Circuits as a hidden quantum layer achieved the highest overall accuracy (OA) of 93.93, and the corresponding F1 score was 0.8477. The Bellman circuit achieved an accuracy of 93.13 with an F1-score of about 0.8248. The classical counterpart of the HQC architecture achieved an overall accuracy of 89.55 with an F1-score of 0.7407. The proposed architecture with two quantum circuits as a hidden layer improved the F1-Score of about 11% (for Bellman Circuit) and 14% (for Real Amplitudes Circuit), respectively, thereby demonstrating the potential of quantum circuits as rich feature descriptors for radar sounder data.

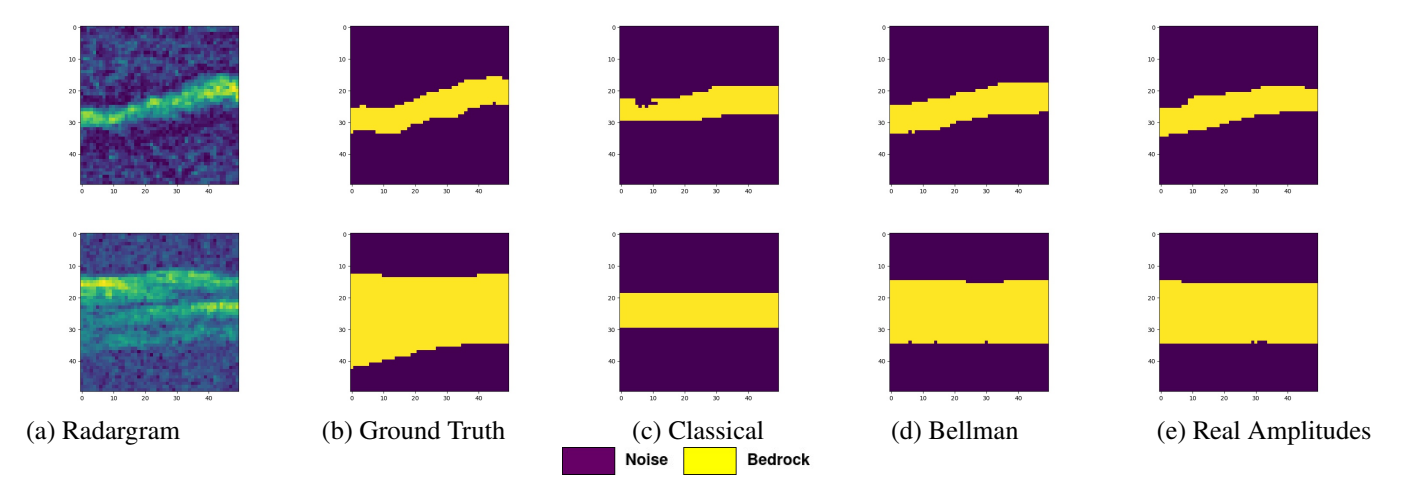


Fig. 6. The Radargram (a), Ground Truth (b), and associated prediction maps are highlighted in this figure (from left to right). (CReSIS. 2023. MCoRDS and MCoRDS3 Data, Lawrence, Kansas, USA. Digital Media. http://data.cresis.ku.edu/.)

Qualitatively, the proposed HQC architecture accurately distinguished the bedrock from the noise for the patch-wise segmentation (see Figure 6). The classical counterpart was unable to distinguish bedrock from noise in several test samples. It was observed that the classical counterpart was unstable during training, whereas, the quantum layer in the latent space successfully stabilized the training. Therefore, the quantum circuits as bottleneck connectors (between the Encoder and Decoder) established a contextually rich back-and-forth information processing system for the UNet-like architecture without using the skip connections in the other part of the networks. While experimenting with the FC layer as a bottleneck connector, the contextual richness of the overall learning mechanism was decreased when discarding the skip connections. Therefore, it would be worth experimenting with the quantum circuits as skip connectors in different parts of the network for a UNET-like Encoder-Decoder architectural setting against the classical skip connectors.

4. CONCLUSIONS

In this work, we explore the potential of QC as a hidden quantum layer for the HQC architecture in the context of radar sounder signal segmentation. The quantum layers demonstrate the capability of achieving the highest accuracy with Real Amplitudes Quantum circuits on the HQC setting, against the classical counterpart. In particular, the F1-score is improved by 14%. However, due to the lack of current hardware infrastructure to handle large-scale quantum circuit-based algorithms, the spatial dimension of the patch size is restricted to 50×50 pixels. In future work, we will explore the experimental setup for the quantum layers as skip connectors for the UNET-like architecture in comparison to the classical skip connectors for investigating the contextual improvement of the overall training with the hybrid setting.

5. REFERENCES

- [1] A. Ilisei and L. Bruzzone, "A system for the automatic classification of ice sheet subsurface targets in radar sounder data," *IEEE TGRS*, vol. 53, pp. 3260–3277, 2015.
- [2] R. Ghosh and F. Bovolo, "Transsounder: A hybrid transunet-transfuse architectural framework for semantic segmentation of radar sounder data," *IEEE TGRS*, vol. 60, pp. 1–13, 2022.
- [3] R. Ghosh and F. Bovolo, "An enhanced unsupervised feature learning framework for radar sounder signal segmentation," in *IGARSS 2023 2023 IEEE IGARSS*, 2023, pp. 6920–6923.
- [4] J. Biamonte, P. Wittek, N. Pancotti, P. Rebentrost, N. Wiebe, and S. Lloyd, "Quantum machine learning," *Nature*, vol. 549, no. 7671, pp. 195–202, Sept. 2017.
- [5] A. Delilbasic, G. Cavallaro, M. Willsch, F. Melgani, M. Riedel, and K. Michielsen, "Quantum support vector machine algorithms for remote sensing data classification," in 2021 IEEE International Geoscience and Remote Sensing Symposium IGARSS, 2021, pp. 2608–2611.
- [6] A. Sebastianelli, D. Zaidenberg, D. Spiller, B. Saux, and S. Ullo, "On circuit-based hybrid quantum neural networks for remote sensing imagery classification," *IEEE JSTARS*, vol. 15, pp. 565–580, 2022.
- [7] F. Fan, Y. Shi, and X. X. Zhu, "Urban land cover classification from sentinel-2 images with quantum-classical network," in *2023 JURSE*, 2023, pp. 1–4.
- [8] M. A. Nielsen and I. L. Chuang, Quantum Computation and Quantum Information, Cambridge University Press, Cambridge, England, Dec. 2010.